© 2013. Published by The Company of Biologists Ltd | Development (2013) 140, 4614-4623 doi:10.1242/dev.096313

RESEARCH ARTICLE

Regulation of maternal Wnt mRNA translation in *C. elegans* embryos

Marieke Oldenbroek[1], Scott M. Robertson[1], Tugba Guven-Ozkan[1,*], Caroline Spike[2], David Greenstein[2] and Rueyling Lin[1,‡]

ABSTRACT

The restricted spatiotemporal translation of maternal mRNAs, which is crucial for correct cell fate specification in early *C. elegans* embryos, is regulated primarily through the 3′UTR. Although genetic screens have identified many maternally expressed cell fate-controlling RNA-binding proteins (RBPs), their *in vivo* targets and the mechanism(s) by which they regulate these targets are less clear. These RBPs are translated in oocytes and localize to one or a few blastomeres in a spatially and temporally dynamic fashion unique for each protein and each blastomere. Here, we characterize the translational regulation of maternally supplied *mom-2* mRNA, which encodes a Wnt ligand essential for two separate cell-cell interactions in early embryos. A GFP reporter that includes only the *mom-2* 3′UTR is translationally repressed properly in oocytes and early embryos, and then correctly translated only in the known Wnt signaling cells. We show that the spatiotemporal translation pattern of this reporter is regulated combinatorially by a set of nine maternally supplied RBPs. These nine proteins all directly bind the *mom-2* 3′UTR *in vitro* and function as positive or negative regulators of *mom-2* translation *in vivo*. The net translational readout for the *mom-2* 3′UTR reporter is determined by competitive binding between positive- and negative-acting RBPs for the 3′UTR, along with the distinct spatiotemporal localization patterns of these regulators. We propose that the 3′UTR of maternal mRNAs contains a combinatorial code that determines the topography of associated RBPs, integrating positive and negative translational inputs.

KEY WORDS: 3′UTR, *Caenorhabditis elegans*, Wnt

INTRODUCTION

Precise patterns of gene expression during development are regulated predominantly at the level of transcription. In transcription-driven gene regulation, transcriptional activators bind to enhancer elements and orchestrate the colocalization of proteins at the gene promoter to activate transcription. The transcriptional status of a particular gene in a cell or developing tissue is therefore determined primarily by the precise combination of transcription factors that can bind to the enhancer sequence in that specific cell.

There are, however, well-known exceptions to transcription-driven gene regulation. Most notably, in newly fertilized embryos of chicken, fish, frog, flies and worms, early cell divisions and fate specification are primarily controlled by proteins and RNAs deposited into the egg by the mother (Newport and Kirschner, 1982; Edgar and Schubiger, 1986; Powell-Coffman et al., 1996). Even in mammals, maternally contributed factors play an essential role early in preimplantation development (Li et al., 2010).

In *C. elegans* embryogenesis, maternal factors control early cleavage events, including their asymmetric nature, orientation and timing, as well as specific cell-to-cell signaling events (Gönczy and Rose, 2005). The first *C. elegans* embryonic division produces two cells of different sizes and developmental potentials. The larger anterior blastomere, termed AB, will generate only somatic tissues, whereas the smaller posterior blastomere, P1, undergoes three more rounds of asymmetric division, each giving rise to a germline precursor (P2, P3 and P4) and a somatic sister blastomere (Fig. 1A).

The asymmetric localization of maternal proteins to restricted blastomeres, which is an essential step in asymmetric divisions and cell fate-specification in early *C. elegans* embryos, is achieved by various mechanisms, including asymmetric distribution, retention and/or degradation (Reese et al., 2000; Hao et al., 2006; Tenlen et al., 2008; Griffin et al., 2011). Maternal factors can also be deposited into the egg as mRNAs and asymmetrically translated in a subset of blastomeres. This provides a way to prevent the precocious activity of powerful developmental regulators and to delimit their functions in a precise spatiotemporal manner. For example, translation of the maternally supplied *zif-1* transcript begins in 4-cell embryos, and then only in somatic blastomeres (Guven-Ozkan et al., 2010; Oldenbroek et al., 2012). ZIF-1 is the substrate-binding subunit of an E3 ligase whose many substrates are enriched in germline blastomeres (DeRenzo et al., 2003). Delayed *zif-1* translation ensures that ZIF-1 protein is present only in cells that have become committed to somatic developmental fates.

Correct spatiotemporal translation of the majority of germline mRNAs in *C. elegans* is controlled via the 3′UTR (Merritt et al., 2008), and we have shown this to be the case for *zif-1* maternal mRNA (Guven-Ozkan et al., 2010; Oldenbroek et al., 2012). Not surprisingly, then, a large proportion of the genes identified through maternal-effect lethal screens as being required for embryonic cell fate specification encode proteins containing RNA-binding motifs (Mello et al., 1994; Draper et al., 1996; Guedes and Priess, 1997; Tabara et al., 1999; Schubert et al., 2000; Gomes et al., 2001). Almost all of these maternally supplied RNA-binding proteins (RBPs) are translated in oocytes, asymmetrically localized after the first mitotic division, and are delimited to one or only a few specific blastomeres following subsequent divisions in a spatially and temporally dynamic fashion that is unique for each protein and each blastomere. Although it is well established that these RBPs are essential for embryogenesis, molecular functions for most of them remain unclear. *In vivo* functional characterization is often complicated by interdependent regulatory

[1]Department of Molecular Biology, University of Texas Southwestern Medical Center, Dallas, TX 75390, USA. [2]Department of Genetics, Cell Biology and Development, University of Minnesota, Minneapolis, MN 55455, USA.
*Present address: Department of Neuroscience, The Scripps Research Institute, Jupiter, FL 33458, USA.

‡Author for correspondence (Rueyling.Lin@UTSouthwestern.edu)

Received 14 March 2013; Accepted 22 August 2013

Development (2013) doi:10.1242/dev.096313

relationships between these RBPs, as well as by the fact that many of them are required for correct blastomere fate specification. RNA binding analyses for several of these proteins have revealed a low sequence specificity for target RNAs, suggesting that specificity *in vivo* might be achieved by combinatorial binding of multiple proteins (Ryder et al., 2004; Pagano et al., 2007; Farley et al., 2008; Pagano et al., 2009).

We showed previously that the correct spatiotemporal translation of maternal *zif-1* mRNA requires seven maternally supplied RBPs: OMA-1, OMA-2, POS-1, SPN-4, MEX-3, MEX-5 and MEX-6 (Oldenbroek et al., 2012). Translation of *zif-1* mRNA is repressed by OMA-1 and OMA-2 in oocytes, by MEX-3 and SPN-4 in 1-cell and early 2-cell embryos, and by POS-1 in germline blastomeres P2-P4. In somatic blastomeres, MEX-5 and MEX-6 relieve translational repression by outcompeting POS-1 for binding to the *zif-1* 3′UTR.

In this study, we characterize the translational regulation of maternally supplied *mom-2* mRNA using a reporter carrying the *mom-2* 3′UTR. *mom-2* encodes a Wnt ligand that is essential for two Wnt-mediated cell-cell interactions during *C. elegans* early embryogenesis (Rocheleau et al., 1997; Thorpe et al., 1997; Park and Priess, 2003; Walston et al., 2004). The first MOM-2/Wnt signal occurs at the 4-cell stage when P2 signals EMS, whereas the second signal occurs at the 8-cell stage when C, the somatic daughter of P2, signals ABar (Fig. 1A). The P2-to-EMS Wnt signal specifies the fate of E, the EMS posterior daughter, as the sole intestinal precursor (Rocheleau et al., 1997; Thorpe et al., 1997; Goldstein, 1992). In embryos deficient in this interaction, E adopts the fate of its sister, MS, which produces no intestinal cells. The Wnt signal from C orients the division axis of ABar toward C (Park and Priess, 2003; Walston et al., 2004). P2 and both P2 daughters, namely C and P3, display MOM-2/Wnt signaling activity, whereas no P2 precursor cells or any other cells at the 4-cell or 8-cell stage do (Park and Priess, 2003). However, the mechanism by which MOM-2 activity is spatially and temporally restricted within the early embryo remained unknown. Here we show that maternally supplied MOM-2/Wnt activity is regulated post-transcriptionally through the *mom-2* 3′UTR. Nine maternal RBPs, many of which were shown previously to also regulate maternal *zif-1* expression, bind the *mom-2* 3′UTR *in vitro* and combinatorially regulate the proper spatiotemporal translation of a *mom-2* 3′UTR reporter *in vivo*. Furthermore, the combinatorial codes are found to be distinct for the expression of the *mom-2* and *zif-1* reporters.

RESULTS

OMA-1 binds to the *mom-2* 3′UTR

OMA-1 and OMA-2 each contain tandem CCCH TIS11-like zinc fingers that can bind to RNAs (Detwiler et al., 2001; Shimada et al., 2002; Jadhav et al., 2008; Li et al., 2009; Guven-Ozkan et al., 2010). OMA-1 and OMA-2 share high sequence similarity and functional redundancy (Detwiler et al., 2001; Shimada et al., 2002) and will be referred to collectively as OMA-1/2 unless stated otherwise. Both proteins are expressed only in oocytes and 1-cell embryos and are degraded soon thereafter. The *oma-1(zu405d)* mutant results in OMA-1 protein persisting past the 1-cell stage, and this OMA-1 persistence underlies its embryonic lethality (Detwiler et al., 2001; Lin, 2003). Approximately 30% of *oma-1(zu405d)* embryos lack intestinal cells, similar to embryos defective in the Wnt pathway (Lin, 2003). This shared phenotype suggests that ectopic OMA-1 in *zu405d* embryos might interfere with the function or expression of one or more components of the Wnt signaling pathway.

In a separate study (to be published elsewhere), we found *mom-2* mRNA to be highly enriched in RNP particles that contain OMA-1 protein. In that study, we introduced a rescuing OMA-1::GFP transgene (*tnIs17*) into the null *oma-1(zu405d te33)* mutant, followed by crossing in the *spe-9(hc88ts)* mutation, which has a temperature-sensitive defect in sperm production. The resulting strain, DG2581, produces normal oocytes but no embryos at 25°C. OMA-1::GFP was pulled down from DG2581 worm lysates using anti-GFP antibody and the co-immunoprecipitated (co-IP) RNAs were analyzed using *C. elegans* Gene Chip Arrays (Affymetrix). *mom-2* mRNA was enriched more than 4-fold in the IP fraction compared with the input RNAs. No RNAs corresponding to other genes known to function in the P2-to-EMS signal, including *mom-1*, *mom-3*, *mom-4*, *mom-5*, *gsk-3*, *apr-1*, *src-1*, *wrm-1* and *lit-1*, were enriched.

The relative abundance of selected transcripts in the OMA-1 IP fraction was also analyzed by RT-qPCR. We assayed *mom-2* transcripts along with *zif-1* and *nos-2* transcripts, which are known targets of OMA-1 (Jadhav et al., 2008; Guven-Ozkan et al., 2010), *pie-1* and *vit-1* transcripts, which are unlikely to be OMA-1 targets, and *mei-1*, an mRNA that is regulated by OMA-1 but only in embryos and not in oocytes (Li et al., 2009). The established targets of OMA protein translational repression during oogenesis (*zif-1* and *nos-2*), as well as *mom-2*, were efficiently recovered compared with negative controls (*pie-1* and *vit-1*) and *mei-1* (Fig. 1B).

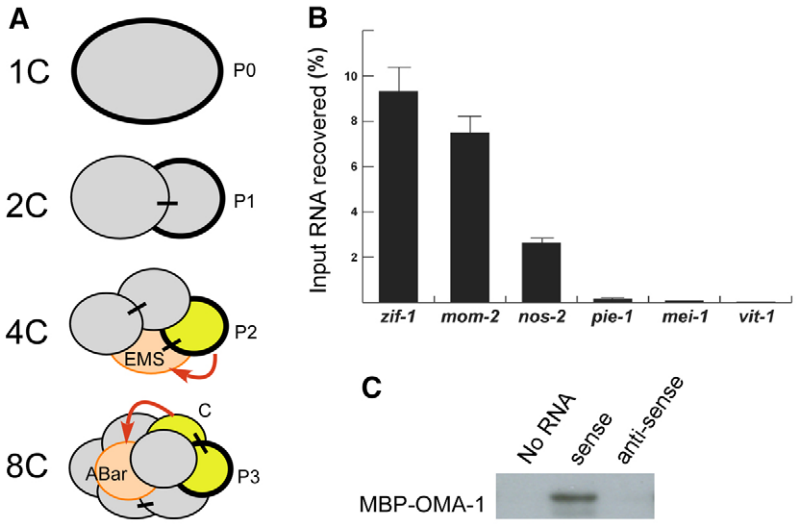

Fig. 1. OMA-1 binds to the *mom-2* 3′UTR *in vitro* and *in vivo*. (A) Illustration of two known MOM-2-dependent interactions (red arrows) in early embryos. Stages of embryos shown in all figures are indicated by the number of blastomeres. Blastomeres exhibiting MOM-2-dependent signaling capability are in yellow. Signal-receiving cells are in orange. Short bars connect sister blastomeres. Germline blastomeres are marked with a thick outline. (B) Recovery of the indicated mRNAs from the input lysate by OMA-1 immunoprecipitation as measured by RT-qPCR. Error bars indicate s.d. (C) *In vitro* RNA pulldown using MBP-OMA-1 and *mom-2* 3′UTR RNA was blotted with anti-MBP antibody.

Development (2013) doi:10.1242/dev.096313

To determine whether the co-IP of *mom-2* mRNA with OMA-1 was due to a direct interaction between the *mom-2* 3′UTR and OMA-1 protein, we performed an *in vitro* RNA binding assay using purified MBP-OMA-1 protein. Following biotinylation, RNA corresponding to the *mom-2* 3′UTR was incubated with MBP-OMA-1 and RNA pulled down with streptavidin-conjugated magnetic beads. The amount of MBP-OMA-1 pulled down with the RNA was analyzed by western blot using an anti-MBP antibody. MBP-OMA-1 was selectively pulled down by RNA corresponding to the sense, but not the antisense, strand of the *mom-2* 3′UTR (Fig. 1C). We conclude that OMA-1 can bind directly to the *mom-2* 3′UTR and therefore might regulate the expression of MOM-2 protein *in vivo*.

The *mom-2* 3′UTR is sufficient to determine the localization pattern of both its mRNA and protein in early embryos

The mechanism by which MOM-2 activity is restricted in early embryos is not known. *mom-2* mRNA was detected in oocytes and early embryos by single-molecule fluorescence *in situ* hybridization (smFISH) (Harterink et al., 2011), which we confirmed (Fig. 2B). We detected uniform *mom-2* mRNA levels in oocytes, 1-cell, 2-cell and early 4-cell embryos. The abundance of *mom-2* mRNA decreases in somatic blastomeres beginning at the late 4-cell stage. By the 12-cell embryo, *mom-2* mRNA was detected at variably decreased levels in different blastomeres but remained relatively unchanged in P3 and C. This preferential degradation in somatic blastomeres has been observed for many, but not all, maternally supplied mRNAs (Seydoux and Fire, 1994).

We generated a reporter construct that expresses nuclear GFP::histone H2B under the control of the germline-specific *pie-1* promoter and the *mom-2* 3′UTR ($P_{pie\text{-}1}$-*gfp::h2b-UTR*$^{mom\text{-}2}$) (Fig. 2A). We will refer to the mRNA and GFP::H2B expressed from $P_{pie\text{-}1}$-*gfp::h2b-UTR*$^{mom\text{-}2}$ as *gfp::h2b*$^{mom\text{-}2}$ and GFP::H2B$^{mom\text{-}2}$, respectively. Using smFISH, *gfp::h2b*$^{mom\text{-}2}$ was detected in oocytes and early embryos in a pattern similar to that of endogenous *mom-2* mRNA (Fig. 2B). Despite *gfp::h2b*$^{mom\text{-}2}$ being detected at a high level in oocytes and early embryos, GFP::H2B$^{mom\text{-}2}$ is not detected until the 4-cell stage, initially at a very low level in the P2 blastomere (Fig. 2B,C). The GFP signal is further elevated in P3 and C, which are the daughters of P2, and remains high in all their subsequent descendants. The strong correlation between the onset of GFP::H2B$^{mom\text{-}2}$ signal and the blastomeres known to exhibit MOM-2 activity argues that the GFP::H2B$^{mom\text{-}2}$ expression pattern closely parallels that of the endogenous maternal MOM-2 protein. Our analysis also suggests that the *mom-2* 3′UTR is sufficient to confer correct localization of both its mRNA and protein in early embryos. Owing to the lack of a good MOM-2 antibody, we characterize here how the expression pattern of GFP::H2B$^{mom\text{-}2}$ is regulated in embryos.

OMA proteins repress GFP::H2B$^{mom\text{-}2}$ expression in oocytes

Repression of GFP::H2B$^{mom\text{-}2}$ expression in oocytes depends on OMA-1/2 proteins. High levels of GFP::H2B$^{mom\text{-}2}$ were observed in oocytes following simultaneous depletion of *oma-1* and *oma-2* by RNAi (Fig. 2C; 100% animals examined, n=50). Furthermore, ectopic OMA-1 appears to be sufficient to repress GFP::H2B$^{mom\text{-}2}$ expression in embryos. In *oma-1(zu405d)* embryos, we observed reduced GFP::H2B$^{mom\text{-}2}$ expression in P3 and C [55±4% (s.d.) reduction in P3, n=13] (Fig. 2B). Translational repression of maternal *mom-2* mRNA by persisting OMA-1 can explain the Wnt phenotype seen in *oma-1(zu405d)* embryos.

We have shown previously that repression of *zif-1* translation by OMA proteins requires the eIF4E-binding protein IFET-1 [previously SPN-2 (Guven-Ozkan et al., 2010)]. IFET-1 binds to both OMA-1 and to the 5′ cap-binding protein eIF4E, presumably creating an inhibitory loop that prevents translation initiation (Li et al., 2009). GFP::H2B$^{mom\text{-}2}$ was derepressed in oocytes of 100% of *ifet-1(RNAi)* animals (n=25) (Fig. 2C), suggesting that OMA proteins also repress translation of *gfp::h2b*$^{mom\text{-}2}$ through an IFET-1-dependent mechanism.

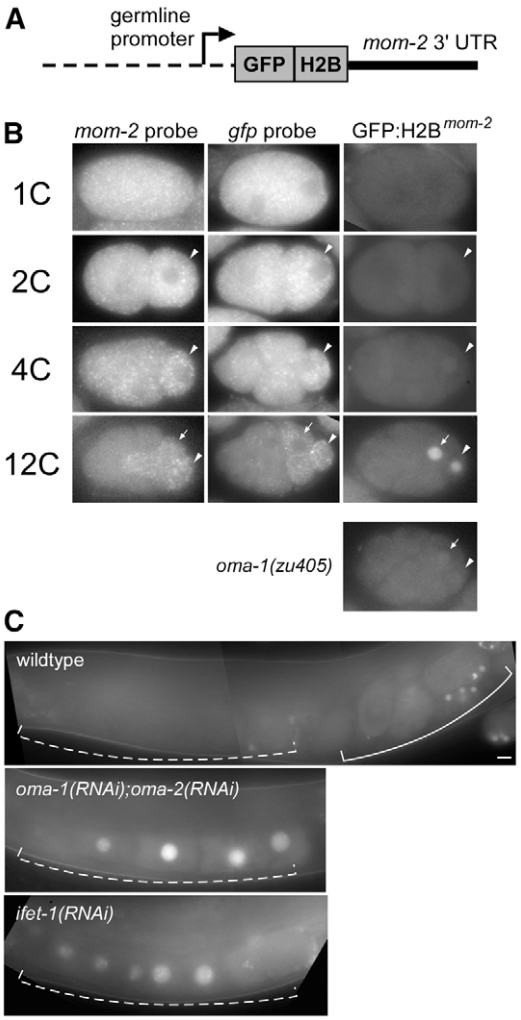

Fig. 2. The *mom-2* 3′UTR is sufficient to determine the localization pattern of *gfp::h2b*$^{mom\text{-}2}$ RNA and GFP::H2B$^{mom\text{-}2}$ protein. (A) Schematic of the reporter construct used. (B) Localization of endogenous *mom-2* (left column) and *gfp::h2b*$^{mom\text{-}2}$ (middle column) mRNAs assayed using smFISH. Right column shows fluorescence micrographs of live embryos expressing GFP::H2B$^{mom\text{-}2}$. A 12-cell *oma-1(zu405d)* embryo is also shown. Arrowheads indicate germline blastomeres; arrows indicate the C blastomere. (C) Fluorescence micrographs of GFP::H2B$^{mom\text{-}2}$ in wild-type, *oma-1/2(RNAi)* and *ifet-1(RNAi)* adult hermaphrodites. Dashed lines indicate oocytes and solid line denotes embryos in the uterus. *oma-1/2(RNAi)* and *ifet-1(RNAi)* animals do not produce embryos. Scale bar: 10 µm.

Together, our *in vitro* and *in vivo* results indicate that OMA-1/2 repress the translation of *gfp::h2b*$^{mom\text{-}2}$, and presumably the *mom-2* mRNA, in oocytes via direct binding to the *mom-2* 3′UTR.

Expression of GFP::H2B$^{mom\text{-}2}$ in early embryos requires MEX-1, PIE-1 and POS-1

OMA proteins are degraded soon after the first mitotic division (Lin, 2003). Therefore, repression by OMA proteins cannot account for

Development (2013) doi:10.1242/dev.096313

the spatiotemporal expression of GFP::H2B$^{mom\text{-}2}$ in embryos. To identify regulators of MOM-2 expression in embryos, we analyzed GFP::H2B$^{mom\text{-}2}$ in embryos depleted individually of specific RBPs. All RBPs tested here are maternally supplied and were initially identified genetically to have essential functions in the fate specification of early blastomeres, which could complicate these analyses. In order to exclude RBPs whose effect on GFP::H2B$^{mom\text{-}2}$ expression could be indirect, possibly via a change in cell fate specification, we first assayed the ability of candidate RBPs to bind to the *mom-2* 3′UTR. We performed a series of *in vitro* RNA binding assays using biotinylated *mom-2* 3′UTR RNA and each candidate RBP. We found that each of these proteins is capable of binding to the *mom-2* 3′UTR in a sense strand-specific manner (Fig. 3A).

We then analyzed GFP::H2B$^{mom\text{-}2}$ levels in embryos individually depleted of these candidate RBPs (Fig. 3B, Fig. 5A). Depletion of any of the three germline blastomere-enriched proteins, MEX-1, PIE-1 and POS-1, resulted in a reduction, but not abolishment, of GFP::H2B$^{mom\text{-}2}$ expression: *mex-1(zu121)*, 50±3% reduction in P3 (n=13); *pie-1(zu154)*, 54±4% reduction in P3 (n=13); *pos-1(zu148)*, 33.1±4% reduction in P3 (n=12). *pos-1(RNAi)* in either the *pie-1(zu154)* or *mex-1(zu121)* strain resulted in no detectable GFP::H2B$^{mom\text{-}2}$ in embryos (n=73 and n=59, respectively). Combined depletion of *pie-1* and *mex-1* [*pie-1(RNAi);mex-1(zu121)*, 55±3% (n=12); *pie-1(zu154);mex-1(RNAi)*, 55±3% (n=12)] did not result in a more severe defect in GFP::H2B$^{mom\text{-}2}$ expression than either single mutant (Fig. 3B; data not shown). smFISH with probes to either *mom-2* or *gfp* mRNA revealed no gross changes in levels in embryos mutant for any of the three genes (supplementary material Fig. S1). We conclude that PIE-1, MEX-1 and POS-1 function together to promote the translation of *gfp::h2b*$^{mom\text{-}2}$ in germline blastomeres.

Embryos depleted of *pie-1*, *mex-1* or *pos-1* exhibit a Wnt signaling-defective phenotype

Reduced expression of GFP::H2B$^{mom\text{-}2}$ could indicate a defect in Wnt-mediated processes in *mex-1*, *pie-1* or *pos-1* mutant embryos. Both *pos-1(zu148)* and *mex-1(zu121)* mutants were previously reported to have endoderm defects (Mello et al., 1992; Tabara et al., 1999). All *pos-1(zu148)* embryos fail to produce endoderm, whereas *mex-1(zu121)* mutant embryos have a cold-sensitive, incompletely penetrant defect in endoderm production. However, the E blastomere in *pos-1(zu148)* or *mex-1(zu121)* embryos does not undergo a homeotic fate change to the MS blastomere, as is also the case for E in *mom-2(or42)* embryos. Specification of MS and the differentiation of MS-derived tissue types requires zygotic transcription (Mango et al., 1994; Broitman-Maduro et al., 2006), which might well be defective in these mutant embryos for reasons unrelated to the translation of maternal *mom-2*. Therefore, we examined ABar division axis realignment, which is a Wnt-dependent event independent of zygotic transcription (Powell-Coffman et al., 1996).

In wild-type embryos, a Wnt signal from the C blastomere aligns the division axis of ABar toward C, perpendicular to the other three AB-derived blastomeres (Park and Priess, 2003; Walston et al., 2004) (Fig. 4A,B). This alignment was shown to be defective in nearly all *mom-2* mutant embryos (Rocheleau et al., 1997; Thorpe et al., 1997), a result we reproduced (96%, n=23). In addition, we observed a similar defect in the ABar division axis in 93% (n=23) of *oma-1(zu405d)*, in 56% (n=27) of *pie-1(zu154)*, in 42% (n=24) of *mex-1(zu121)* and in 44% (n=16) of *pos-1(zu148)* embryos. This defect was enhanced when one of the other two positive regulators was also depleted by RNAi in *mex-1(zu121)* or *pos-1(zu148)* embryos. There was only modest or no enhancement when RNAi was combined with *pie-1(zu154)* embryos (Table 1). Although our results suggest that defective Wnt/MOM-2 translation underlies the spindle orientation defect in *pos-1*, *mex-1* and *pie-1* mutant embryos, we cannot rule out the possibility of an indirect effect. For example, P2 (and its descendants) is not properly specified in the *pie-1* or *pos-1* mutant. Furthermore, in the *mex-1* mutant the AB lineage develops with irregular timing (Schnabel et al., 1996) and the ABar fate is changed (Mello et al., 1992; Tabara et al., 1999).

MEX-3/5/6 and SPN-4 repress *gfp::h2b*$^{mom\text{-}2}$ translation in embryos

In vivo analyses showed that the RBPs MEX-3, SPN-4, MEX-5 and MEX-6 have repressive roles in the expression of GFP::H2B$^{mom\text{-}2}$. These four proteins are all present at a high levels in oocytes and 1-cell embryos, but are subsequently asymmetrically localized to different subsets of blastomeres (Draper et al., 1996; Schubert et al., 2000; Ogura et al., 2003). Depletion of *spn-4* or *mex-3* resulted in GFP::H2B$^{mom\text{-}2}$ expression as early as the 1-cell stage (supplementary material Fig. S2), and in all subsequent blastomeres

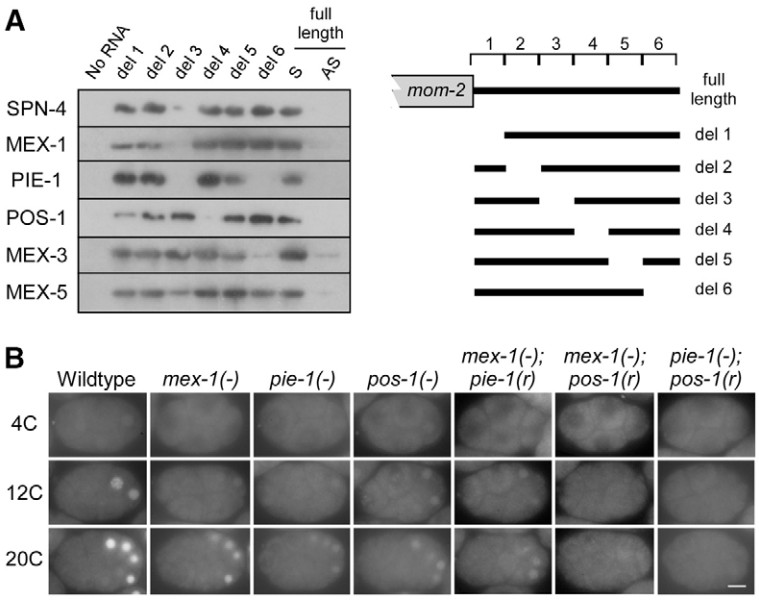

Fig. 3. MEX-1, PIE-1 and POS-1 promote GFP::H2B$^{mom\text{-}2}$ expression. (A) *In vitro* RNA pulldowns using RNAs corresponding to either the full-length or deleted versions (del1-del6) of the *mom-2* 3′UTR as illustrated on the right. S and AS denote sense and antisense RNAs, respectively. POS-1, SPN-4, MEX-1, MEX-3 and MEX-5 were assayed using anti-MBP antibody, whereas PIE-1 was assayed using anti-Flag antibody. (B) Fluorescence micrographs of live embryos expressing GFP::H2B$^{mom\text{-}2}$ in mutant (–) or RNAi (r) backgrounds. Scale bar: 10 µm.

Development (2013) doi:10.1242/dev.096313

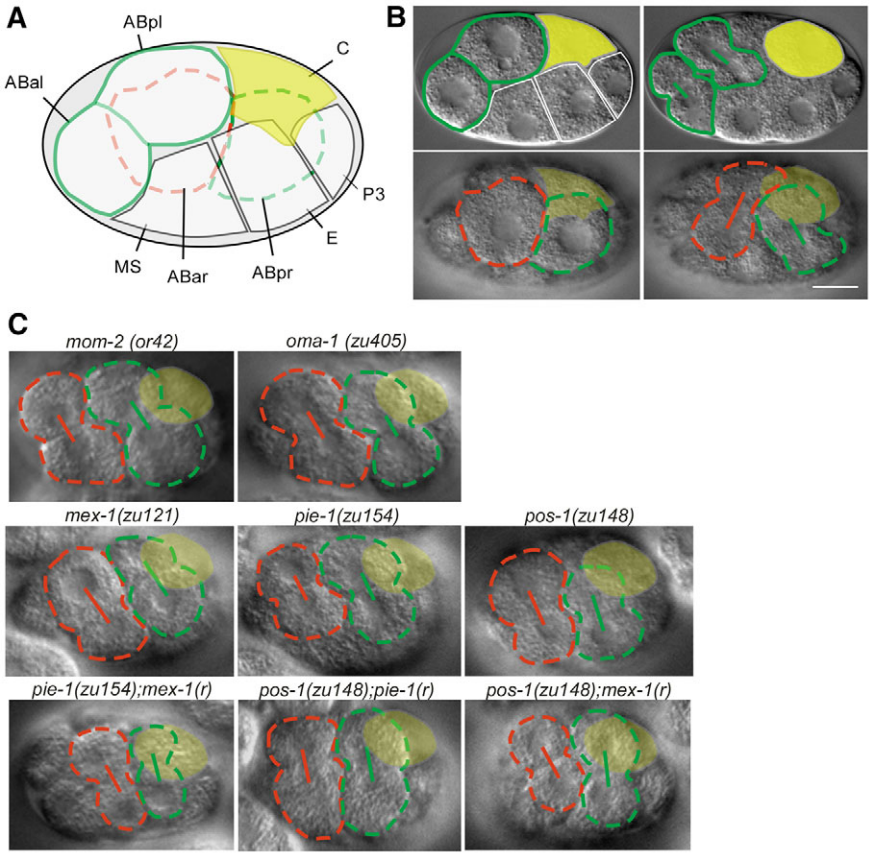

Fig. 4. Embryos depleted of *pie-1*, *mex-1* or *pos-1* exhibit a Wnt signaling-defective phenotype. (A) Schematic of a wild-type 8-cell embryo. Solid and dashed outlines indicate blastomeres on two different focal planes. ABar is outlined in red, with all other AB descendants outlined in green. Yellow, C blastomere. (B) (Left column) DIC images of two different focal planes of a wild-type 8-cell embryo. (Right column) The four AB descendants in the same embryos undergoing division. (C) DIC micrographs showing division axes of ABar and ABpr in embryos with the indicated mutations or RNAi (r) treatment. Scale bar: 10 μm.

(Fig. 5A). No GFP::H2B$^{mom\text{-}2}$ was detected in oocytes of *mex-3(RNAi)* or *spn-4(RNAi)* animals (not shown). These results suggest that SPN-4 and MEX-3 are both required for the translational repression of *gfp::h2b*$^{mom\text{-}2}$ in the 1-cell embryo.

MEX-5 and MEX-6 share high sequence similarity, exhibit identical expression patterns and function redundantly in nearly all cases when assayed *in vivo* (Schubert et al., 2000). Both proteins are highly enriched in AB after the first mitotic division, and localize to all three somatic blastomeres, but not P2, in the 4-cell embryo. In *mex-5(RNAi);mex-6(RNAi)* embryos, we observed uniform expression of GFP::H2B$^{mom\text{-}2}$ in all blastomeres as early as the 4-cell stage (Fig. 5A). The spatial localization of MEX-5/6, the derepression of GFP::H2B$^{mom\text{-}2}$ in *mex-5/6(RNAi)* embryos, and the *in vitro* binding of the *mom-2* 3′UTR by MEX-5, all suggest that MEX-5/6 directly repress translation of *gfp::h2b*$^{mom\text{-}2}$ mRNA in somatic blastomeres. MEX-5/6 activity is not required for *gfp::h2b*$^{mom\text{-}2}$ translational repression until the 4-cell stage.

Depletion of either *spn-4* or *mex-5/6* resulted in *mom-2* and *gfp::h2b*$^{mom\text{-}2}$ mRNAs being uniformly distributed in embryos beyond the 4-cell stage (Fig. 5B; supplementary material Fig. S1), likely the result of defective degradation of these mRNAs in somatic blastomeres. Whereas ectopic *gfp::h2b*$^{mom\text{-}2}$ mRNA may contribute to the ectopic expression of GFP::H2B$^{mom\text{-}2}$ in 4-cell and older embryos, it cannot account for the ectopic expression of GFP::H2B$^{mom\text{-}2}$ in 1- or 2-cell embryos, in which *gfp::h2b*$^{mom\text{-}2}$ is already high in wild-type embryos.

In *mex-5(RNAi);mex-6(RNAi)* embryos, PIE-1, MEX-1 and POS-1 are all uniformly localized (Schubert et al., 2000). However, uniform localization of all three positive regulators is not the cause of the uniform expression of GFP::H2B$^{mom\text{-}2}$ observed in *mex-5(RNAi);mex-6(RNAi)* embryos. Simultaneous depletion of *pie-1* and *pos-1* [*(pie-1(zu154);pos-1(RNAi)*] or of *mex-1* and *pos-1* [*mex-1(zu121);pos-1(RNAi)*] in *mex-5(RNAi);mex-6(RNAi)* embryos resulted in no change to the uniform expression of GFP::H2B$^{mom\text{-}2}$ (Fig. 5A; supplementary material Fig. S3). Similarly, PIE-1, MEX-1 and POS-1 are not required for the GFP::H2B$^{mom\text{-}2}$ derepression observed in *mex-3(RNAi)* or *spn-4(RNAi)* embryos (Fig. 5A; supplementary material Fig. S3). The observation that the positive regulators PIE-1, MEX-1 and POS-1 are not required for GFP::H2B$^{mom\text{-}2}$ expression when negative regulators are depleted suggests that these positive regulators promote the expression of GFP::H2B$^{mom\text{-}2}$ by antagonizing the negative regulators.

MEX-3 binds IFET-1, an eIF4E-binding protein

The GFP::H2B$^{mom\text{-}2}$ expressed in oocytes of *ifet-1(RNAi)* animals persists into embryos, precluding a determination of whether IFET-1 activity is also required for the repression of *mom-2* in embryos. We did, however, investigate whether any of the RBPs functioning in the embryo bind to IFET-1 *in vitro*. Like MBP-OMA-1, MBP-MEX-3 efficiently pulled down His-IFET-1 in an *in vitro* pulldown assay (Fig. 5C). Low, but reproducible, amounts of His-IFET-1 were also pulled down by MBP-MEX-1. No detectable IFET-1 was pulled down with any of the other proteins tested. This suggests that the repression of *gfp::h2b*$^{mom\text{-}2}$ translation in embryos by MEX-3 is through a mechanism involving IFET-1, similar to the translational repression by OMA-1/2 in oocytes.

Competitive binding of maternal RBPs to the *mom-2* 3′UTR determines GFP::H2B$^{mom\text{-}2}$ expression

The seven regulators of GFP::H2B$^{mom\text{-}2}$ expression in embryos are themselves provided as maternal proteins and are all present in the

Development (2013) doi:10.1242/dev.096313

Table 1. Percentage of embryos with a defective ABar division axis

Genotype	Defective ABar division axis (%)	*n*
Wild type	0	23
pie-1(–)	56	27
pie-1(–);mex-1(r)	63	30
pie-1(–);pos-1(r)	69	16
mex-1(–)	42	24
mex-1(–);pie-1(r)	67	27
mex-1(–);pos-1(r)	84	25
pos-1(–)	44	16
pos-1(–);mex-1(r)	79	19
pos-1(–);pie-1(r)	73	15
oma-1(zu405)	93	23
mom-2(or42)	96	23

1-cell embryo. Beginning with the first embryonic division, these seven proteins exhibit dynamic and different spatiotemporal localization patterns (Fig. 6A) (Draper et al., 1996; Mello et al., 1996; Guedes and Priess, 1997; Tabara et al., 1999; Schubert et al., 2000; Ogura et al., 2003). To better understand how translation of *gfp::h2b*$^{mom\text{-}2}$ transcripts is determined in cells possessing a combination of both positive and negative regulators, we performed the following two sets of experiments. First, we divided the *mom-2* 3′UTR into six equal regions in order to map binding sites for each protein. We generated *mom-2* 3′UTR RNAs deleted for one of the six regions (del1-del6 RNAs) and performed binding assays with each of the RBPs (Fig. 3A). SPN-4, MEX-1 and PIE-1 binding was abolished with del3 RNA, suggesting that region 3 contains sequence essential for their binding. PIE-1 binding appears to require sequence present in region 6 as well. The same assay revealed that regions 4 and 6 are essential for POS-1 and MEX-3 binding, respectively. Region 4 and region 6 contain a predicted POS-1 and MEX-3 binding site, respectively (supplementary material Fig. S4) (Farley et al., 2008; Pagano et al., 2009). Consistent with multiple putative MEX-5 binding sites across the entire *mom-2* 3′UTR, no single region was found to be essential for MEX-5 binding (Fig. 7D; supplementary material Fig. S4) (Farley et al., 2008; Pagano et al., 2009).

Second, we performed *in vitro* RNA binding competition experiments. Both a positive and a negative regulator were mixed with the target biotinylated *mom-2* 3′UTR RNA to determine whether binding of one protein is favored over the other. P2 and P3 have a high level of the negative regulator SPN-4, as well as the three positive regulators PIE-1, MEX-1 and POS-1 (Fig. 6A). We found that mixing MEX-1 or PIE-1 with SPN-4 immediately prior to the addition of *mom-2* 3′UTR RNA resulted in the binding of only MEX-1 or PIE-1, but not SPN-4, to the RNA. This result and the above 3′UTR domain mapping suggest that PIE-1 and MEX-1 share overlapping binding sites with SPN-4 and that binding of either protein prevents simultaneous binding by SPN-4. In P2 and P3, the high level of MEX-1 and PIE-1 presumably prevents SPN-4 from binding to the *mom-2* 3′UTR, thereby antagonizing the SPN-4 repressive effect. In a similar competition RNA binding experiment, we found that binding of POS-1 and SPN-4 to the *mom-2* 3′UTR RNA was not affected by the presence of the other protein, consistent with the domain mapping showing that these two proteins bind to distinct regions of the 3′UTR (Fig. 3A, Fig. 6B).

EMS, the somatic sister of P2, does not express GFP::H2B$^{mom\text{-}2}$. Levels of SPN-4, MEX-1, POS-1, MEX-5 and MEX-6 are all initially high in EMS, whereas the first three proteins are degraded by the proteasome later in the cell cycle (Fig. 6A). We found that when MEX-1 or POS-1 was pre-mixed with MEX-5 in the RNA binding reaction, only MEX-5, but not MEX-1 or POS-1, was pulled down by the *mom-2* 3′UTR RNA (Fig. 6C). The clear binding preference for MEX-5 over MEX-1 or POS-1, along with the persistence of MEX-5/6 levels in EMS can explain the repression of *gfp::h2b*$^{mom\text{-}2}$ translation in EMS. The competition assay showed no preference in binding to the *mom-2* 3′UTR RNA for MEX-3 versus MEX-1 or POS-1 (Fig. 6D), consistent with these three proteins binding preferentially to different regions as shown in Fig. 3A.

DISCUSSION

We show here that a large set of maternally supplied RBPs is required to set up proper MOM-2/Wnt signaling in the *C. elegans* embryo, thereby specifying normal intestinal development and spindle orientation. The 3′UTR of the *mom-2* transcript is sufficient to confer localization information for both the *gfp::h2b*$^{mom\text{-}2}$ mRNA

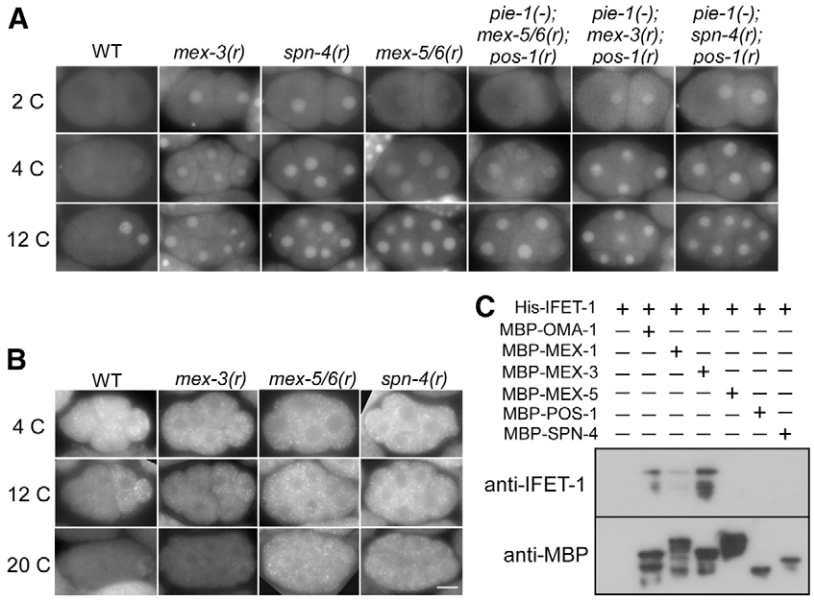

Fig. 5. MEX-3, SPN-4 and MEX-5/6 repress GFP::H2B$^{mom\text{-}2}$ expression. Fluorescence micrographs (A) or smFISH images with *gfp* probe (B) of embryos expressing GFP::H2B$^{mom\text{-}2}$ in various RNAi (r) or mutant (–) backgrounds. (C) His-IFET-1 was mixed with individual MBP-tagged proteins and pulled down with amylose beads. Proteins pulled down were assayed using the indicated antibodies. Scale bar: 10 µm.

Development (2013) doi:10.1242/dev.096313

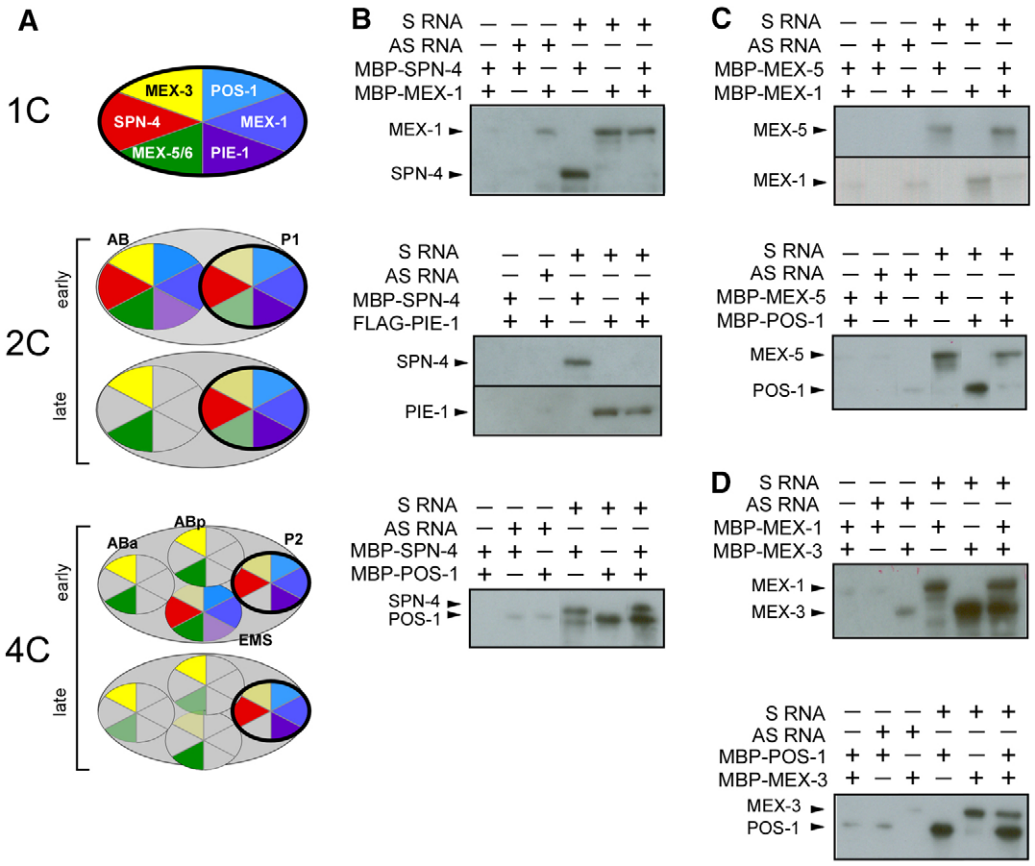

Fig. 6. Competitive binding to *mom-2* 3′UTR RNA.
(A) Schematic of MEX-3 (yellow), SPN-4 (red), MEX-5/6 (green), POS-1 (aqua), MEX-1 (blue) and PIE-1 (purple) localization in early embryos at the indicated stages. Each protein is represented in each blastomere by a 1/6 section of that blastomere where shading indicates protein levels. Germline blastomeres are in thick outline. (B-D) Competition *mom-2* 3′UTR RNA binding assays. S and AS denote sense and antisense RNAs, respectively.

and the corresponding GFP::H2B$^{mom\text{-}2}$ protein. The *gfp::h2b*$^{mom\text{-}2}$ mRNA is translationally repressed properly in oocytes and early embryos, and correctly translated in known Wnt signaling cells. We have identified nine maternally supplied RBPs that can all bind *in vitro* to an RNA corresponding to the *mom-2* 3′UTR and that suffice to explain the correct spatiotemporal translation of *gfp::h2b*$^{mom\text{-}2}$ transcripts *in vivo*. *In vitro* experiments reveal overlapping binding sites and a hierarchy of binding preferences to the *mom-2* 3′UTR among these RBPs.

Common themes governing translational control via the 3′UTR

Our studies on the *mom-2* and *zif-1* (Oldenbroek et al., 2012) 3′UTRs reveal two common mechanisms for how positive and negative regulators control translation of these maternal mRNAs via the 3′UTR. First, in the absence of all positive and negative regulators identified to date, the transcripts are translated. Unless additional positive regulator(s) required for translation of *gfp::h2b*$^{mom\text{-}2}$ are identified, our results suggest that these maternal mRNAs are inherently capable of being translated. Repression of each transcript in oocytes and embryos is maintained by spatially and temporally distinct sets of repressors. Translation occurs when repression is relieved or antagonized by a positive regulator (Fig. 7A). Our results suggest competitive binding of 3′UTR sequences as a likely mechanism for relieving translational repression *in vivo*. We cannot, however, rule out additional mechanisms by which positive-acting RBPs could interfere with repression, such as by binding and sequestering a negative-acting RBP or by masking binding sites for inhibitory microRNAs. Second, the spatiotemporal translational readout of a reporter appears to be controlled by the combination of competitive binding between positive- and negative-acting RBPs for specific 3′UTR sequences and the blastomere-specific localization of particular RBPs.

Translational control in oocytes

We show that OMA-1/2 are required in oocytes to repress *gfp::h2b*$^{mom\text{-}2}$ mRNA translation, and are capable of continued repression when ectopically present in post-1-cell embryos. This can explain the Wnt-defective phenotype associated with *oma-1(zu405d)* embryos (Fig. 7A). These results also explain the curious phenotypes of *gsk-3(RNAi)* and *gsk-3(nr2047ts)* embryos. In the canonical Wnt pathway, GSK-3 negatively regulates the pathway by phosphorylating β-catenin and promoting its degradation (Wu and Pan, 2010). However, *gsk-3(RNAi)* and *gsk-3(nr2047ts)* embryos partially resemble *mom-2* mutant embryos, for both β-catenin-dependent and β-catenin-independent phenotypes, suggesting a positive role upstream of β-catenin in the *C. elegans* Wnt pathway (Schlesinger et al., 1999; Shirayama et al., 2006). We and others have shown that *gsk-3(RNAi)* and *gsk-3(nr2047ts)* embryos express ectopic OMA-1 protein, which is likely to underlie their Wnt-defective phenotypes (Nishi and Lin, 2005; Shirayama et al., 2006). Our demonstration here that OMA proteins repress the translation of *gfp::h2b*$^{mom\text{-}2}$ suggests that previously characterized Wnt-defective phenotypes in *gsk-3(RNAi)* and *gsk-3(nr2047ts)* embryos are likely the result of compromised expression of the Wnt/MOM-2 ligand (Fig. 7C).

Translational control in 1- and 2-cell embryos

Repression of *gfp::h2b*$^{mom\text{-}2}$ translation in 1- and 2-cell embryos requires both SPN-4 and MEX-3 (Fig. 7A,B). We showed

Development (2013) doi:10.1242/dev.096313

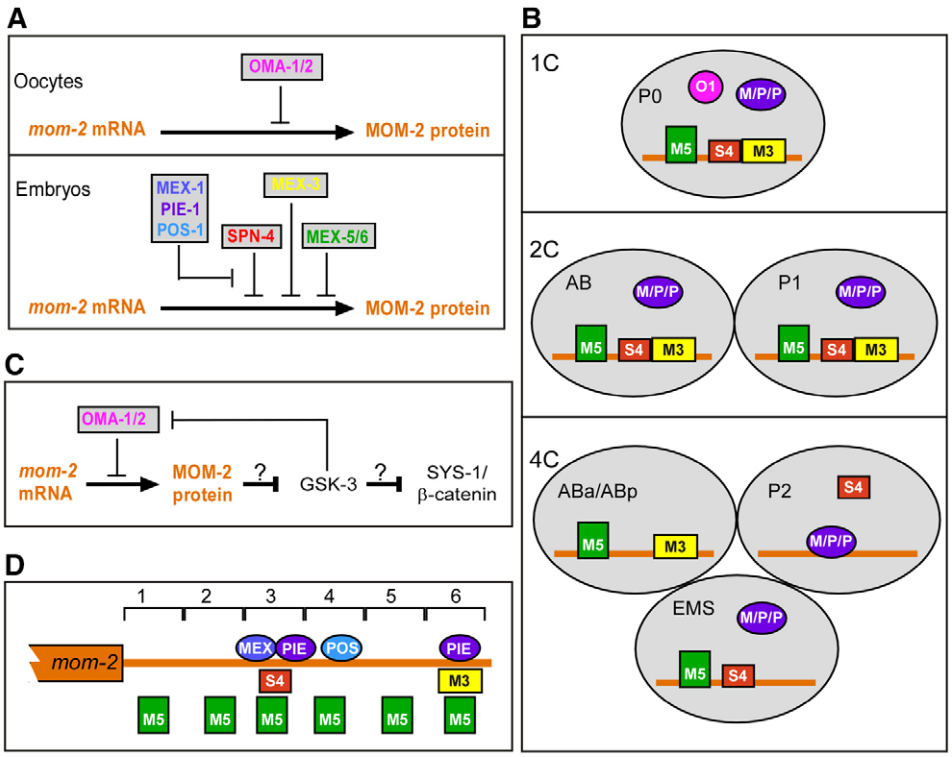

Fig. 7. Model of maternal *mom-2* translational control. (A) Proposed functions of each tested RBP in the translation of *mom-2* mRNA in oocytes and embryos. MEX-1, PIE-1 and POS-1 positively regulate *mom-2* translation via antagonizing repression by the other proteins. (B) Proposed regulation of *mom-2* translation in each early blastomere (gray ovals) as a result of the hierarchical binding of the tested regulators. O1, OMA-1; M/P/P, MEX-1, PIE-1 and POS-1; M5, MEX-5/6; S4, SPN-4; M3, MEX-3. Brown line, *mom-2* 3′UTR. (C) The function of GSK-3 in a canonical Wnt signaling pathway and the proposed negative-feedback loop between GSK-3, OMA-1/2 and *mom-2* translation. Question marks denote regulations that have not been demonstrated in *C. elegans* embryos. (D) Schematic of the *mom-2* 3′UTR and proposed binding regions of each protein based on the *in vitro* mapping data shown in Fig. 3A.

previously that repression of the *zif-1* 3′UTR reporter in early germline blastomeres also requires both MEX-3 and SPN-4 (Oldenbroek et al., 2012). In *spn-4(RNAi);mex-3(zu155)* embryos, the *zif-1* reporter is expressed precociously as early as the 2-cell stage. High levels of both MEX-3 and SPN-4 coexist within the same cell only in the 1-cell and (briefly) early 2-cell embryo (Draper et al., 1996; Ogura et al., 2003), thereby limiting translational repression of their joint targets to only these very early stages. Repression would be relieved after the 2-cell stage when MEX-3 and SPN-4 no longer coexist. This distinctive mode of translational repression highlights the unique molecular nature of the 1-cell embryo, with protein regulators of different developmental pathways coexisting within a common cytoplasm with maternally supplied mRNAs that need to be translated in a blastomere-restricted manner (Robertson and Lin, 2013).

We show that MEX-3 can bind to IFET-1, suggesting a possible mechanism by which MEX-3 could inhibit *mom-2* translation (Guven-Ozkan et al., 2010). MEX-3, bound to the *mom-2* 3′UTR, and IFET-1, bound to the 5′ cap (Li et al., 2009), could form a closed loop that inhibits translation through a IFET-1–MEX-3 interaction. SPN-4 has been shown to physically interact with MEX-3 (Huang et al., 2002; Ogura et al., 2003) and therefore it is possible that SPN-4 also represses translation of MEX-3 target mRNAs by stabilizing an inhibitory loop involving MEX-3 and IFET-1.

Translational control after the 2-cell stage

In 4-cell embryos, high levels of SPN-4 and MEX-3 are detected in reciprocal patterns, with SPN-4 in both P2 and EMS, and MEX-3 in ABa and ABp (Fig. 6A) (Draper et al., 1996; Ogura et al., 2003). The P2 blastomere also has high levels of MEX-1, PIE-1 and POS-1. A low level of MEX-3 in conjunction with the competitive binding advantage of PIE-1 and MEX-1 over SPN-4 can explain why *mom-2* is translated in P2 (Fig. 7A,B). Two observations suggest that POS-1 promotes translation of *gfp::h2b*$^{mom\text{-}2}$ mRNA through a mechanism different from that by MEX-1 and PIE-1. First, whereas both PIE-1 and MEX-1 share overlapping binding sites with SPN-4, POS-1 appears to bind to a different region. Second, *pos-1* RNAi in either *pie-1* or *mex-1* mutant embryos enhances the defects in GFP::H2B$^{mom\text{-}2}$ expression. By contrast, little or no enhancement was observed following simultaneous depletion of *mex-1* and *pie-1*. With the caveat that this conclusion is based on experiments using RNAi, it is consistent with POS-1 repressing translation of *gfp::h2b*$^{mom\text{-}2}$ mRNA through a mechanism that differs from that of MEX-1 and PIE-1.

Our data suggest a model in which the repression of *mom-2* translation in EMS results from high levels of MEX-5/6, coupled with their competitive binding advantage over MEX-1 and POS-1 for the *mom-2* 3′UTR. The MEX-5 binding advantage could derive from higher numbers of putative binding sites in the *mom-2* 3′UTR (supplementary material Fig. S4). In addition, MEX-5/6 could contribute to *mom-2* translational repression in somatic blastomeres in at least two other ways. First, MEX-5/6 activity is required to keep the level of *mom-2* mRNA low in somatic blastomeres, probably by promoting its degradation. Second, it has been shown that MEX-5/6 activity is required to restrict PIE-1, MEX-1 and POS-1 to the germline blastomeres (Schubert et al., 2000).

Intriguingly, whereas POS-1 and MEX-5/6 have essential and antagonistic roles in regulating maternal *zif-1* and *mom-2* translation, they function in opposite ways on each transcript (Oldenbroek et al., 2012). POS-1 is a negative regulator for *zif-1* translation in P2. The preference for MEX-5/6 binding to the 3′UTR over POS-1 appears to drive translation of *zif-1* in EMS. The contrary is true for *mom-2*, where POS-1 promotes translation in P2 and MEX-5/6 represses translation in EMS. It is currently unclear how POS-1 and MEX-5/6 can exhibit opposite functions within the same cell in the translational regulation of different maternal transcripts.

3′UTRs as post-transcriptional enhancers

In newly fertilized embryos, regulating gene expression at the level of translation provides certain advantages over transcriptional regulation.

Development (2013) doi:10.1242/dev.096313

First, it uncouples protein expression from transcription, which needs to be repressed for correct specification of germline blastomeres in both flies and worms (Nakamura and Seydoux, 2008). Second, because it does not require transcription, translational control is faster and therefore much better suited to a developmental program in which cell divisions occur every 10-15 minutes.

The importance of 3′UTRs and the RBPs bound to them in regulating the translation of germline transcripts is well established in *C. elegans* and *Drosophila* (Wilkie et al., 2003; Piccioni et al., 2005; Merritt et al., 2008). However, the mechanism by which the cohort of maternally supplied RBPs specifies cell fate in early *C. elegans* embryos via the translational regulation of multiple shared targets remains largely unknown. Our results here lead us to propose that the 3′UTR of maternal mRNAs contains a combinatorial code that determines the precise topography of RBPs, both positive and negative, that are bound to it. Therefore, the spatiotemporal expression pattern of any particular maternal mRNA is determined primarily by the precise combination of RNA-binding regulators present in the cell that are capable of binding to the 3′UTR sequence. By reading the combinatorial code provided by the 3′UTR, this cohort of RBPs specifies cell fate through translational control. This is reminiscent of transcriptional enhancers, whose binding sites provide a combinatorial code for cell-specific regulators that specify cell fate through transcriptional control. Future studies will more precisely define the combinatorial code(s) associated with maternal mRNAs, as well as interrogating RBP codes associated with somatic transcripts.

MATERIALS AND METHODS

Strains

Genetic markers used were: LGI, *spe-9(hc88ts)*; LGII, *mex-1(zu121), teIs127($P_{pie\text{-}1}$-gfp::h2b-UTR$^{mom\text{-}2}$)*; LGIII, *unc-119(ed3)*, *pie-1(zu154)*; LGIV, *oma-1(zu405d), oma-1(zu405d te33)*; LGV, *oma-2(te51), pos-1(zu148), tnIs17[unc-119(+), pCS410 (oma-1:s:tev:gfp)]*. Strains used are: TX1377 *teIs127($P_{pie\text{-}1}$-gfp::h2b-UTR$^{mom\text{-}2}$)*, DG2460 *spe-9(hc88ts); oma-1(zu405d te33)*, DG2581 *spe-9(hc88ts); oma-1(zu405d te33); tnIs17,* DG2620 *unc-119(ed3); oma-1(zu405d te33); oma-2(te51); tnIs17. tnIs17* rescues *oma-1(zu405d te33); oma-2(te51)* sterility. All integrated lines were generated by bombardment (Praitis et al., 2001).

Plasmid construction

Most plasmids were constructed using Gateway technology (Guven-Ozkan et al., 2010). A 557 bp genomic sequence beginning 100 bp upstream of the *mom-2* stop codon was cloned downstream of *pie-1* promoter-driven GFP::H2B in the vector pID3.01B (Guven-Ozkan et al., 2010; Reese et al., 2000). pCS410 was created by modifying plasmid pRL475 (Lin, 2003). DNA encoding a codon-optimized S tag and tobacco etch virus (TEV) protease cleavage site was created using gene synthesis (Hoover and Lubkowski, 2002) and ligated into a *Nhe*I site created between OMA-1 and GFP coding sequence.

RNAi and imaging

Feeding RNAi was performed by feeding L1 larvae for 2 days at 25°C (Timmons and Fire, 1998). All images were acquired, processed and quantified as described previously (Guven-Ozkan et al., 2008). Spindle orientation was assayed using sequential DIC *z*-stacks.

smFISH

CAL590-coupled probes were purchased from Biosearch Technologies and hybridization was performed as described (Raj and Tyagi, 2010) with a few modifications as follows. Embryos were collected by cutting adult hermaphrodites on poly-lysine-coated slides, squashed with a coverslip, incubated in 3.7% formaldehyde for 15 minutes, and frozen on dry ice. Upon removal of the coverslip, embryos were treated with 95% ethanol for 10 minutes at −20°C, fresh 95% ethanol for 5 minutes at room temperature, 70% ethanol for 3 hours at 4°C, 400 µl wash buffer for 10 minutes, then 100 µl probe (0.1 µM) overnight at 37°C, followed by three 20-minute washes in wash buffer at 37°C, and then mounted.

Recombinant proteins and RNA binding assays

Maltose binding protein (MBP)-tagged proteins and HIS-IFET-1 were purified from *E. coli* and Flag-PIE-1 was purified from HeLa cells (Li et al., 2009; Oldenbroek et al., 2012). Biotinylation of RNA and pulldowns were performed as described (Lee and Schedl, 2001; Guven-Ozkan et al., 2010). The optimal amounts of purified protein and *mom-2* 3′UTR RNA were empirically determined by titration. A typical binding reaction contained 150 ng purified protein (34.5, 30.3, 34.1, 31.5, 41.5, 36.7 and 76.3 nM, respectively, for MBP-tagged OMA-1, MEX-1, MEX-3, MEX-5, POS-1, SPN-4 and Flag-PIE-1) and 400 ng biotinylated RNA. For the competition binding assays, RNA was kept limiting compared with proteins used (1 µg each MBP-tagged protein and 130 ng RNA, except for the SPN-4/PIE-1 competition, where 750 ng MBP-SPN-4 and 400 ng FLAG-PIE-1 were used).

Purification of OMA-1 and associated RNAs from adult worms

OMA-1:S:TEV:GFP was purified as described (Cheeseman et al., 2004; Cheeseman and Desai, 2005) with modifications. Young adults were sonicated in 50 mM HEPES (pH 7.5), 100 mM KCl, 1 mM $MgCl_2$, 10% glycerol, 0.05% NP40, and protease inhibitors (complete EDTA-free, Roche). OMA-1:S:TEV:GFP was purified from 1 ml medium-speed supernatant [18,000 ***g***/2×10 minutes, supplemented to 300 mM KCl and 200 units RNasin (Promega)] with 20 µg anti-GFP antibody (NB600-308, Novus Biologicals) cross-linked to 150 µl Dynabeads protein A (Invitrogen) at 4°C for 1 hour. Dynabeads were washed seven times with IP wash buffer (sonication buffer supplemented to 300 mM KCl, 20 units/ml RNasin, 5 mM 2-mercaptoethanol, 5 mM sodium citrate, 10 µM $ZnCl_2$) before incubation with 0.25 units/µl AcTEV protease (Invitrogen) overnight at 4°C to release immunoprecipitated OMA-1:S protein. RNAs were purified from this supernatant (IP RNA) or from 50 µl of crude lysate (input RNA) using Trizol (Invitrogen) and precipitated with linear acrylamide (Sigma).

RT-qPCR

RT-qPCR was performed on IP and input RNA samples from the same DG2581 lysate and an IP RNA sample from a similarly prepared DG2460 lysate, which lacks the OMA-1:S:TEV:GFP fusion protein. Reverse transcription was performed with IP RNA or input RNA using SuperScript II reverse transcriptase (Invitrogen) and random primers according to the manufacturer's instructions [oligo(dT) primers performed similarly]. qPCR was performed using FastStart SYBR Green Master Mix (Roche) on a Mastercycler ep realplex instrument (Invitrogen) in triplicate with appropriate controls. Fold enrichment relative to the mock IP and estimated percentage of input RNA were calculated as $2^{-[Ct(IP)-Ct(mock\ IP)]}$ and $100\{2^{-[Ct(IP)-Ct(input,\ corrected)]}\}$, respectively. In the latter calculation, the raw Ct value of the input sample was corrected to account for the fact that 0.8% of input sample was used for each RT-PCR reaction. Only fold enrichment relative to input RNA is shown in Fig. 1.

Acknowledgements

We thank R.L. laboratory members and Michael Buszczak for discussions; Drs Priess, Seydoux and Rose for reagents; and the Caenorhabditis Genetics Center (CGC) [NIH P40 OD010440] for strains.

Competing interests

The authors declare no competing financial interests.

Author contributions

S.M.R. and R.L. designed the project. T.G.-O. contributed to early results. M.O. performed the experiments pertaining to *in vitro* and *in vivo* RBP binding to the *mom-2* 3′UTR. C.S. and D.G. designed and performed the co-immunoprecipitation of OMA-1 bound RNAs from embryos. S.M.R. and R.L. wrote the paper.

Funding

This work was supported by National Institutes of Health (NIH) grants [HD37933 and GM84198] to R.L., NIH grants [GM57173 and GM65115] to D.G., and a

Genetics Training Grant [5T32GM083831] to M.O. Deposited in PMC for release after 12 months.

Supplementary material

Supplementary material available online at
http://dev.biologists.org/lookup/suppl/doi:10.1242/dev.096313/-/DC1

References

Broitman-Maduro, G., Lin, K. T., Hung, W. W. and Maduro, M. F. (2006). Specification of the C. elegans MS blastomere by the T-box factor TBX-35. *Development* **133**, 3097-3106.

Cheeseman, I. M. and Desai, A. (2005). A combined approach for the localization and tandem affinity purification of protein complexes from metazoans. *Sci. STKE* **2005**, pl1.

Cheeseman, I. M., Niessen, S., Anderson, S., Hyndman, F., Yates, J. R., 3rd, Oegema, K. and Desai, A. (2004). A conserved protein network controls assembly of the outer kinetochore and its ability to sustain tension. *Genes Dev.* **18**, 2255-2268.

DeRenzo, C., Reese, K. J. and Seydoux, G. (2003). Exclusion of germ plasm proteins from somatic lineages by cullin-dependent degradation. *Nature* **424**, 685-689.

Detwiler, M. R., Reuben, M., Li, X., Rogers, E. and Lin, R. (2001). Two zinc finger proteins, OMA-1 and OMA-2, are redundantly required for oocyte maturation in C. elegans. *Dev. Cell* **1**, 187-199.

Draper, B. W., Mello, C. C., Bowerman, B., Hardin, J. and Priess, J. R. (1996). MEX-3 is a KH domain protein that regulates blastomere identity in early C. elegans embryos. *Cell* **87**, 205-216.

Edgar, B. A. and Schubiger, G. (1986). Parameters controlling transcriptional activation during early Drosophila development. *Cell* **44**, 871-877.

Farley, B. M., Pagano, J. M. and Ryder, S. P. (2008). RNA target specificity of the embryonic cell fate determinant POS-1. *RNA* **14**, 2685-2697.

Goldstein, B. (1992). Induction of gut in Caenorhabditis elegans embryos. *Nature* **357**, 255-257.

Gomes, J. E., Encalada, S. E., Swan, K. A., Shelton, C. A., Carter, J. C. and Bowerman, B. (2001). The maternal gene spn-4 encodes a predicted RRM protein required for mitotic spindle orientation and cell fate patterning in early C. elegans embryos. *Development* **128**, 4301-4314.

Gönczy, P. and Rose, L. S. (2005) Asymmetric cell division and axis formation in the embryo. *WormBook* **2005** Oct 15:1-20.

Griffin, E. E., Odde, D. J. and Seydoux, G. (2011). Regulation of the MEX-5 gradient by a spatially segregated kinase/phosphatase cycle. *Cell* **146**, 955-968.

Guedes, S. and Priess, J. R. (1997). The C. elegans MEX-1 protein is present in germline blastomeres and is a P granule component. *Development* **124**, 731-739.

Guven-Ozkan, T., Nishi, Y., Robertson, S. M. and Lin, R. (2008). Global transcriptional repression in C. elegans germline precursors by regulated sequestration of TAF-4. *Cell* **135**, 149-160.

Guven-Ozkan, T., Robertson, S. M., Nishi, Y. and Lin, R. (2010). zif-1 translational repression defines a second, mutually exclusive OMA function in germline transcriptional repression. *Development* **137**, 3373-3382.

Hao, Y., Boyd, L. and Seydoux, G. (2006). Stabilization of cell polarity by the C. elegans RING protein PAR-2. *Dev. Cell* **10**, 199-208.

Harterink, M., Kim, D. H., Middelkoop, T. C., Doan, T. D., van Oudenaarden, A. and Korswagen, H. C. (2011). Neuroblast migration along the anteroposterior axis of C. elegans is controlled by opposing gradients of Wnts and a secreted Frizzled-related protein. *Development* **138**, 2915-2924.

Hoover, D. M. and Lubkowski, J. (2002). DNAWorks: an automated method for designing oligonucleotides for PCR-based gene synthesis. *Nucleic Acids Res.* **30**, e43.

Huang, N. N., Mootz, D. E., Walhout, A. J., Vidal, M. and Hunter, C. P. (2002). MEX-3 interacting proteins link cell polarity to asymmetric gene expression in Caenorhabditis elegans. *Development* **129**, 747-759.

Jadhav, S., Rana, M. and Subramaniam, K. (2008). Multiple maternal proteins coordinate to restrict the translation of C. elegans nanos-2 to primordial germ cells. *Development* **135**, 1803-1812.

Lee, M. H. and Schedl, T. (2001). Identification of in vivo mRNA targets of GLD-1, a maxi-KH motif containing protein required for C. elegans germ cell development. *Genes Dev.* **15**, 2408-2420.

Li, W., DeBella, L. R., Guven-Ozkan, T., Lin, R. and Rose, L. S. (2009). An eIF4E-binding protein regulates katanin protein levels in C. elegans embryos. *J. Cell Biol.* **187**, 33-42.

Li, L., Zheng, P. and Dean, J. (2010). Maternal control of early mouse development. *Development* **137**, 859-870.

Lin, R. (2003). A gain-of-function mutation in oma-1, a C. elegans gene required for oocyte maturation, results in delayed degradation of maternal proteins and embryonic lethality. *Dev. Biol.* **258**, 226-239.

Mango, S. E., Lambie, E. J. and Kimble, J. (1994). The pha-4 gene is required to generate the pharyngeal primordium of Caenorhabditis elegans. *Development* **120**, 3019-3031.

Mello, C. C., Draper, B. W., Krause, M., Weintraub, H. and Priess, J. R. (1992). The pie-1 and mex-1 genes and maternal control of blastomere identity in early C. elegans embryos. *Cell* **70**, 163-176.

Mello, C. C., Draper, B. W. and Priess, J. R. (1994). The maternal genes apx-1 and glp-1 and establishment of dorsal-ventral polarity in the early C. elegans embryo. *Cell* **77**, 95-106.

Mello, C. C., Schubert, C., Draper, B., Zhang, W., Lobel, R. and Priess, J. R. (1996). The PIE-1 protein and germline specification in C. elegans embryos. *Nature* **382**, 710-712.

Merritt, C., Rasoloson, D., Ko, D. and Seydoux, G. (2008). 3′ UTRs are the primary regulators of gene expression in the C. elegans germline. *Curr. Biol.* **18**, 1476-1482.

Nakamura, A. and Seydoux, G. (2008). Less is more: specification of the germline by transcriptional repression. *Development* **135**, 3817-3827.

Newport, J. and Kirschner, M. (1982). A major developmental transition in early Xenopus embryos: I. characterization and timing of cellular changes at the midblastula stage. *Cell* **30**, 675-686.

Nishi, Y. and Lin, R. (2005). DYRK2 and GSK-3 phosphorylate and promote the timely degradation of OMA-1, a key regulator of the oocyte-to-embryo transition in C. elegans. *Dev. Biol.* **288**, 139-149.

Ogura, K., Kishimoto, N., Mitani, S., Gengyo-Ando, K. and Kohara, Y. (2003). Translational control of maternal glp-1 mRNA by POS-1 and its interacting protein SPN-4 in Caenorhabditis elegans. *Development* **130**, 2495-2503.

Oldenbroek, M., Robertson, S. M., Guven-Ozkan, T., Gore, S., Nishi, Y. and Lin, R. (2012). Multiple RNA-binding proteins function combinatorially to control the soma-restricted expression pattern of the E3 ligase subunit ZIF-1. *Dev. Biol.* **363**, 388-398.

Pagano, J. M., Farley, B. M., McCoig, L. M. and Ryder, S. P. (2007). Molecular basis of RNA recognition by the embryonic polarity determinant MEX-5. *J. Biol. Chem.* **282**, 8883-8894.

Pagano, J. M., Farley, B. M., Essien, K. I. and Ryder, S. P. (2009). RNA recognition by the embryonic cell fate determinant and germline totipotency factor MEX-3. *Proc. Natl. Acad. Sci. USA* **106**, 20252-20257.

Park, F. D. and Priess, J. R. (2003). Establishment of POP-1 asymmetry in early C. elegans embryos. *Development* **130**, 3547-3556.

Piccioni, F., Zappavigna, V. and Verrotti, A. C. (2005). A cup full of functions. *RNA Biol.* **2**, 125-128.

Powell-Coffman, J. A., Knight, J. and Wood, W. B. (1996). Onset of C. elegans gastrulation is blocked by inhibition of embryonic transcription with an RNA polymerase antisense RNA. *Dev. Biol.* **178**, 472-483.

Praitis, V., Casey, E., Collar, D. and Austin, J. (2001). Creation of low-copy integrated transgenic lines in Caenorhabditis elegans. *Genetics* **157**, 1217-1226.

Raj, A. and Tyagi, S. (2010). Detection of individual endogenous RNA transcripts in situ using multiple singly labeled probes. *Methods Enzymol.* **472**, 365-386.

Reese, K. J., Dunn, M. A., Waddle, J. A. and Seydoux, G. (2000). Asymmetric segregation of PIE-1 in C. elegans is mediated by two complementary mechanisms that act through separate PIE-1 protein domains. *Mol. Cell* **6**, 445-455.

Robertson, S. and Lin, R. (2013). The oocyte-to-embryo transition. *Adv. Exp. Med. Biol.* **757**, 351-372.

Rocheleau, C. E., Downs, W. D., Lin, R., Wittmann, C., Bei, Y., Cha, Y. H., Ali, M., Priess, J. R. and Mello, C. C. (1997). Wnt signaling and an APC-related gene specify endoderm in early C. elegans embryos. *Cell* **90**, 707-716.

Ryder, S. P., Frater, L. A., Abramovitz, D. L., Goodwin, E. B. and Williamson, J. R. (2004). RNA target specificity of the STAR/GSG domain post-transcriptional regulatory protein GLD-1. *Nat. Struct. Mol. Biol.* **11**, 20-28.

Schlesinger, A., Shelton, C. A., Maloof, J. N., Meneghini, M. and Bowerman, B. (1999). Wnt pathway components orient a mitotic spindle in the early Caenorhabditis elegans embryo without requiring gene transcription in the responding cell. *Genes Dev.* **13**, 2028-2038.

Schnabel, R., Weigner, C., Hutter, H., Feichtinger, R. and Schnabel, H. (1996). mex-1 and the general partitioning of cell fate in the early C. elegans embryo. *Mech. Dev.* **54**, 133-147.

Schubert, C. M., Lin, R., de Vries, C. J., Plasterk, R. H. and Priess, J. R. (2000). MEX-5 and MEX-6 function to establish soma/germline asymmetry in early C. elegans embryos. *Mol. Cell* **5**, 671-682.

Seydoux, G. and Fire, A. (1994). Soma-germline asymmetry in the distributions of embryonic RNAs in Caenorhabditis elegans. *Development* **120**, 2823-2834.

Shimada, M., Kawahara, H. and Doi, H. (2002). Novel family of CCCH-type zinc-finger proteins, MOE-1, -2 and -3, participates in C. elegans oocyte maturation. *Genes Cells* **7**, 933-947.

Shirayama, M., Soto, M. C., Ishidate, T., Kim, S., Nakamura, K., Bei, Y., van den Heuvel, S. and Mello, C. C. (2006). The conserved kinases CDK-1, GSK-3, KIN-19, and MBK-2 promote OMA-1 destruction to regulate the oocyte-to-embryo transition in C. elegans, *Curr. Biol.* **16**, 47-55.

Tabara, H., Hill, R. J., Mello, C. C., Priess, J. R. and Kohara, Y. (1999). pos-1 encodes a cytoplasmic zinc-finger protein essential for germline specification in C. elegans. *Development* **126**, 1-11.

Tenlen, J. R., Molk, J. N., London, N., Page, B. D. and Priess, J. R. (2008). MEX-5 asymmetry in one-cell C. elegans embryos requires PAR-4- and PAR-1-dependent phosphorylation. *Development* **135**, 3665-3675.

Thorpe, C. J., Schlesinger, A., Carter, J. C. and Bowerman, B. (1997). Wnt signaling polarizes an early C. elegans blastomere to distinguish endoderm from mesoderm. *Cell* **90**, 695-705.

Timmons, L. and Fire, A. (1998). Specific interference by ingested dsRNA. *Nature* **395**, 854.

Walston, T., Tuskey, C., Edgar, L., Hawkins, N., Ellis, G., Bowerman, B., Wood, W. and Hardin, J. (2004). Multiple Wnt signaling pathways converge to orient the mitotic spindle in early C. elegans embryos. *Dev. Cell* **7**, 831-841.

Wilkie, G. S., Dickson, K. S. and Gray, N. K. (2003). Regulation of mRNA translation by 5′- and 3′-UTR-binding factors. *Trends Biochem. Sci.* **28**, 182-188.

Wu, D. and Pan, W. (2010). GSK3: a multifaceted kinase in Wnt signaling. *Trends Biochem. Sci.* **35**, 161-168.